Aug 11th - Aug 16th

Nonlinear Seismic Analysis of Buried Pipelines During Liquefaction

Amir M. Halabian
Isfahan University of Technology, Isfahan, Iran

S. Hamid Hashemolhosseini
Isfahan University of Technology, Isfahan, Iran

Mehdi Rezaei
Isfahan University of Technology, Isfahan, Iran


6th International Conference on
Case Histories in Geotechnical Engineering, Arlington, VA, August 11-16, 2008

NONLINEAR SEISMIC ANALYSIS OF BURIED PIPELINES DURING LIQUEFACTION

Amir M. Halabian
Faculty of Civil Engineering
Isfahan University of Technology
Isfahan, Iran

S. Hamid Hashemolhosseini
Faculty of Mining Engineering
Isfahan University of technology
Isfahan, Iran

Mehdi Rezaei
Faculty of Civil Engineering
Isfahan University of technology
Isfahan, Iran

ABSTRACT

The safety of buried pipelines during earthquakes has involved a great deal of attention in last few years. Important characteristics of buried pipelines are that they cover large areas and can be subjected to a variety of geotectonic hazards. Earthquake damages to buried pipelines can be attributed to transient ground deformations (TGD), permanent ground deformations (PGD) or both. PGD occurs as a result of surface faulting, liquefaction, landslides, and differential settlement from consolidation of cohesionless soil. To evaluate seismic behavior of buried pipelines subjected to large values of permanent ground deformations, appropriate non-linear cyclic stress-strain relationship should be implemented in any numerical method. Among the phenomena, which cause permanent ground deformations, the settlement and lateral spreading induced by liquefaction are considered as the main cause of damage in buried structures. Therefore, this study is aimed to take into account the potential of liquefaction during an earthquake into the numerical analysis of buried pipelines using FEM. During the earthquake, the soil volume and also pore-pressure water is changed and therefore as saturated loose sands undergo simple shear deformations, the stiffness at any time is changed as the function of mean normal effective stress. In this study, a hypo-elastic model is adopted for the soil to evaluate changes in the pore pressures and also effective stresses during the excitation. In a finite element modeling, for the areas not expecting the liquefaction to occur, the pipe is modeled using beam elements and soil is modeled by some bi-linear springs; while for liquefied areas, the pipe is modeled by shell elements and solid elements are used to model the surrounding soil.

INTRODUCTION

A great deal of study has been done regarding the safety of buried pipelines in the last few years. Since buried pipeline networks cover wide areas, therefore they may be subjected to a variety of geotectonic hazards including spatial ground motions. A number of severe earthquakes in recent years such as 1995 Kobe in Japan, the 1999 Chi-Chi in Taiwan and the 1999 Kocaeli in Turkey have shown that the damage mechanism of buried pipelines could be mainly caused by post-earthquake hazards such as fault movement, land sliding and also liquefaction-induced soil displacements all so-called Permanent Ground Deformation (PGD). Therefore performance of buried pipelines may significantly be affected by permanent ground deformations during and after earthquake. The widespread soil liquefaction that happened in Japan during the 1995 Hyogoken-Nambu earthquake (Kobe earthquake) caused tremendous damage to various lifeline facilities resulting flotation of buried pipelines. Since then serious concern to buried pipelines was realized by researchers due to damages occurred resulting from liquefaction as one of cause of permanent ground deformation.

A detailed review of the literature on earthquake response of underground pipeline systems reveals that great progress has been acquired (O'Rourke and Lane (1989)) in seismic response of buried pipelines subjected to fault movement. The pseudo-static method has been used widely in analyzing the soil-pipe mutual system. This method only models the soil as springs simply, and cannot consider the reduction of soil intensity. Under a seismic action for saturated sands, because of the remarkable nonlinear behavior and the solid-liquid two-phase character of the soil, the dynamic properties of the soil will be changed significantly and the deformation of soil is mostly depended on the development of pore water pressure. This nonlinear cyclic behavior of the soil may influence the dynamic response of the soil-pipeline system.

This study focused primarily on pipeline response resulting from earthquake deformation induced by liquefaction. Therefore, the effect of soil cyclic nonlinear behavior, introduced by soil liquefaction, on the soil-pipe interaction phenomena is evaluated throughout a time history analysis. Knowing this fact that implementing advanced constitutive

models into any dynamic numerical analysis method requires remarkable computational efforts, a very simple algorithm to define the hysteretic loops when liquefiable sands are subjected to ground motions during loading-reloading phase of excitation is developed. A practical diameter of Gas pipelines embedded in different soil layers are chosen to reveal the unfavorable effects of the soil-structure interaction phenomenon during liquefaction. Using the simple hysteretic algorithm for saturated soils developed here in this study, a 3D coupled finite element modeling is carried out to trace the stresses and deformations of the pipe and the adjacent soil during the initial liquefaction. For a given site, appropriate input ground motions are chosen to enforce the inelastic behavior of the soil. The role of several parameters on both the pipe's response and induced soil strains are extensively studied. In a framework of parametric studies, the present work can be extended to the different soil profiles and properties as well as the characteristics of the input motion (i.e. amplitude, frequency content, Arias intensity).

CONSTITUTIVE MODEL FOR LIQUEFIABLE SOIL

The earthquake response of saturated sands is a very complicated process due to coupling between the dissipation and the re-distribution of pore water pressure and also the soil frame deformation during cyclic loading. Dynamic shear stresses and shear strain generated by the earthquake cause slip at grain contacts and then the volume could be changed and consequently the pore-pressure during the event may be increased until all effective stresses are eliminated from the system. In this state the sand has significant loss of shearing resistance and deform like a liquid. Therefore, one can say that the soil shear modulus of elasticity at a given strain level is a function of normal effective stresses. As a result, when computing the response of saturated sands to a given earthquake, important factors can be classified as: the soil initial shear modulus, the variation of shear modulus with shear strain and generation and dissipation of pore-water pressures. To simulate the liquefaction, the soil in the model should be assumed to show the hysteretic characteristics based on the undrained conditions. Therefore, it is very important to consider the hysteretic characteristics on the effective stress-strain relationships of soils. In this study, the constitutive law developed by Finn and Lee (1977) as a hypo-elastic model was employed to evaluate the shear modulus of elasticity as a function of effective shear stress or shear strain. The skeleton curve is given by the following hyperbolic equation (Fig. 1):

$$\tau = \frac{G_{m0}}{\left(1 + G_{m0}\,\gamma / \tau_{m0}\right)}\gamma \qquad (1)$$

As seen in Fig. 1, G_{m0} is the shear modulus at the initial part of the backbone curve and τ_{m0} is the undrained shear strength, both can be obtained by Hardin-Dernevich relation (Prakash, 1981):

$$G_{m0} = \alpha \frac{(2.973 - e)^2}{1+e}.\left(\frac{1+2k_0}{3}\right)^{1/2}.\sqrt{\sigma_v'} \qquad (2)$$

$$\tau_{m0} = \left[\left(\frac{1+K_0}{2}\,Sin\phi'\right)^2 - \left(\frac{1+K_0}{2}\right)^2\right]^{1/2}\sigma_v' \qquad (3)$$

where e, σ_v', K_0 and ϕ' are void ratio, effective vertical stress, confining pressure ratio and soil friction angle, respectively.

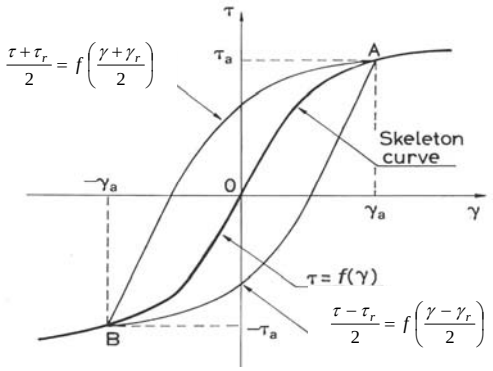

Fig. 1. Soil stress-strain relationship

For each loading-reloading loop, after reversal point, the unloading path is defined as

$$\frac{\tau - \tau_r}{2} = f\left(\frac{\gamma - \gamma_r}{2}\right) \qquad (4)$$

in which τ_r and γ_r are the shear stress and shear strain at the reversal point. During the liquefaction as the effective stress and soil stiffness decreases, the effect of increased pore pressure is to degrade or soften the soil backbone curve. In the Finn constitutive model, relating the pore pressure variations to the incremental volumetric strain, the rebound shear modulus is expressed as

$$G_{mn} = G_{m0}\left(\frac{\sigma_v'}{\sigma_{v0}'}\right)^{1/2} \qquad (5)$$

where σ_v' and σ_{v0}' are the current and initial vertical effective stresses. To take into account effect of degrading in the undrained shear strength for the nth cycle, τ_{mn}, can also be evaluated as

$$\tau_{mn} = \tau_{m0}\left(\frac{\sigma_v'}{\sigma_{v0}'}\right) \qquad (6)$$

In this study, an energy dissipation approach was used to modify the Finn model and to predict the reversal point in loading-reloading paths of hysteretic loop. Based on this approach the reversal loading direction is judged by the sign of the dissipated energy increment (the incremental shear work), ΔW_S. The shear work increment can be obtained in a FEM analysis as the different between the total incremental work, ΔW_T, and the incremental volumetric work, ΔW_N, for an increment strain during loading or reloading as

$$\Delta W_s = \Delta W_T - \Delta W_N \quad (7)$$

where

$$\Delta W_T = \sigma_{11}\Delta\varepsilon_{11} + \sigma_{22}\Delta\varepsilon_{22} + \sigma_{33}\Delta\varepsilon_{33} + 2(\sigma_{12}\Delta\varepsilon_{12} + \sigma_{13}\Delta\varepsilon_{13} + \sigma_{23}\Delta\varepsilon_{23})$$

(8)

$$\Delta W_N = \tfrac{1}{3} \cdot \sum_{K=1}^{K=3} \sigma_{KK}\Delta\varepsilon_{KK} \quad (9)$$

The rebound shear modulus can be calculated by effective stresses through a non-linear dynamic analysis. However, in the effective stress analysis the results strongly depend on the constitutive equations and also the level of effective vertical stresses at the different loading-reloading cycles. Therefore in this study, the energy dissipation approach was also used to evaluate the maximum shear modulus at the initial part of each loading-reloading loop as:

$$G_{mn} = G_{m0}.(1-(\frac{W_s}{W_T})^m) \quad (10)$$

where W_s is the total shear work and W_T is the total work done to the n^{th} cycle. The parameter m will be obtained throughout a calibration process with the experimental works. The variation of the excess pore water pressure can be obtained using the definition of the effective stress, i.e.

$$U = \sigma_v - \sigma_v' \quad (11)$$

The effective stress at a given time, *t*, can also be evaluated by

$$\frac{\sigma_{v0}'}{\sigma_v'} = \left(\frac{G_{m0}}{G_t}\right)^2 \quad (12)$$

As it was mentioned the model proposed in this study is a simple model that characterize only liquefaction aspect of saturated sands behavior. Hence, the model parameters should be defined from standard undrained triaxial tests. The implementation of the proposed model in a finite element code has been tested by simulation of a triaxial compression test with initial confining pressure, p', equal to 212 kPa (Habte, 2006). The experimental tests was for the soil with initial void ratio of 0.737 and internal friction angle of 30^0. Using the finite element code equipped with the proposed non-linear soil constitutive model proposed in this study, an axi-symmetric FE model was developed (shown in Fig. 2). The results for the above triaxial test for deviatoric stress versus shear strain are shown in Fig. 3, which is matched with the results reported in Fig. 4 (Habte, 2006) in terms of the maximum stress and the number of loops.

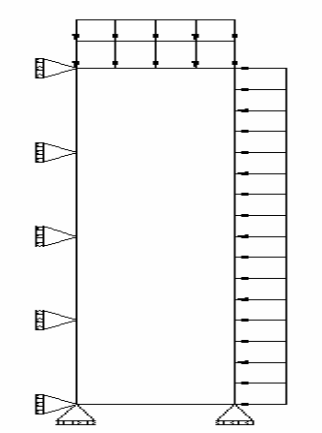

Fig. 2. The triaxial test FE model

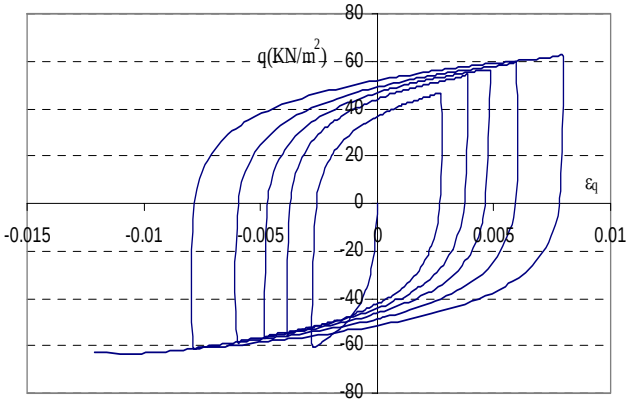

Fig. 3. Cyclic undrained triaxial FE model q-ε_q curve

SOIL-PIPE MODELING

The early studies on buried pipelines behavior subjected to permanent ground deformation specially fault movements were focused on the displacements that cause tensile failure of the pipeline using cable theory (Newmark-Hall, 1975; Kennedy, 1977). Some observations of the damages (V-shape and Z-shape) caused by earthquakes showed that pipelines could undergo out of plane axial and bending deformations due to ground displacements specially when crossing normal faults and in plane axial and bending deformations at reverse faults. Since the cable theory could not satisfy the equilibrium condition for a pipeline crossing a reverse fault, the beam model was developed to consider the bending stiffness of the pipe (Wang and Yeh 1985). In the beam model, the large deflection part of the pipe was modeled as a constant curvature curved segment and the remaining part of the pipe, which is small deflection, was treated as a semi-infinite beam on elastic foundation. For the cases that the pipe is subjected to moderate and large movements, this model yielded more realistic than cable model. It has been noticed from past earthquakes that the buried pipelines suffered severe damages

due to huge deformations in the pipe section that creates the very large amount of strain. Therefore, the pipe response in some areas is a complicated nonlinear behavior. Since it is difficult for the cable or beam model to analyze the large deformation in the pipe crossing section, the shell FEM model has been proposed in the analysis of fault-crossing pipeline in order to consider the effect of local buckling and wrinkle in the pipe's section (Ariman and Lee, 1992). In this study to investigate the effect large deformation in the pipe's sections and also non-linear behavior of liquefiable soil during earthquake a hybrid shell-beam model was adapted to represents the long geometry of soil-pipe system. In this finite element model, the middle part located in the area susceptible to liquefaction has been modeled by shell elements for the pipe and 8-node brick elements for the soil around the pipe. While beam elements are used for the side parts, which are between the fixed point and end points of the shell segment

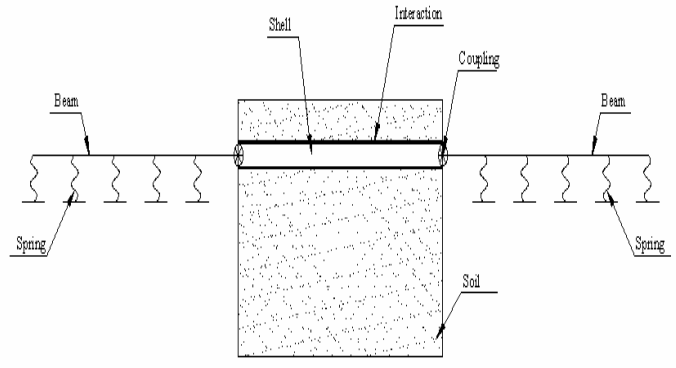

Fig. 4. Soil-pipeline system

displacement between the soil and pipe increases (Trautmann and O'Rourke, 1983). However, in this study as the side parts and are subjected to large deformations in the soil-pipe system (Fig. 4). To assess the integrity of the pipelines against ground deformations, it is important to quantitatively evaluate the interaction between the pipelines and the surrounding soil. The shell elements are linked with beam elements to represent sections of straight pipe outside the zone of large localized strain induced by liquefaction. Soil-pipeline interaction in the side parts in response to relative displacement between pipe and soil is modeled with discrete spring elements using a bilinear force-displacement relationship to represent the elasto-plastic nature of the soil-pipeline interaction. Theses springs represent the axial, transverse horizontal and transverse vertical soil restraints. The soil-pipeline interaction specified in the major seismic design guidelines for pipelines has a bilinear force-displacement relationship curve, where the actual experimental results showed due to large ground deformations the soil-pipe interaction decreases as the relative are subjected less deformation, using bilinear representations are sufficiently adequate.

Using the load-deformation characteristics for soil-pipeline interaction recommended in ALA, the parameters for mutually perpendicular Winkler's springs are obtained from Table 1. In the Table 1, D and H are the pipe's diameter and embedded depth, respectively. C is the soil cohesion and $\bar{\gamma}$ is used as effective unit weight. N_{ch} and N_{qh} can be obtained from the

Table 1. Bilinear soil-pipeline interaction springs parameters [7]

Component	Ultimate soil force	Yield soil displacement
Axial (t-x curves)	$t_u = \pi D \alpha C + \pi D H \bar{\gamma} \frac{1+K_0}{2} \tan\delta$ $\alpha = 0.608 - 0.123C - \frac{0.274}{C^2+1} + \frac{0.695}{C^3+1}$	$\Delta_t = 0.05 \quad cm$
Transverse Horizontal(p-y curves)	$p_u = N_{ch} CD + N_{qh} \bar{\gamma} HD$	$\Delta_P = 0.04(H + D/2) \le (0.1 - 0.15)D$
Transverse Vertical (q-z curves)	Upward Direction: $Q_u = \begin{cases} N_{cv} C_u D & for\ Clays \\ N_{qv} \bar{\gamma} HD & for\ Sands \end{cases}$ $N_{cv} = 2(H/D) \le 10$ $N_{qv} = (\frac{\varphi H}{44\ D}) \le N_q$ Downward Direction: $Q_d = N_c CD + N_q \bar{\gamma} HD + N_\gamma \gamma \frac{D^2}{2}$	Upward Direction: For Sands: $\Delta q_u = (0.01-0.02)H < 0.1D$ For Clays: $\Delta q_u = (0.1-0.2)H < 0.2D$ Downward Direction: For Sands: $\Delta q_u = 0.1D$ For Clays: $\Delta q_u = 0.2D$

charts recommended by ALA (2001). N_c, N_q and N_γ are the soil capacity factors given by ALA (2001).

THE GOVERNING EQUATIONS

The displacements and tractions within the soil around the pipe and also inside the pipe are obtained from the governing equation

$$\begin{bmatrix} \mathbf{M}_{pp} & \mathbf{0} & \mathbf{0} \\ \mathbf{0} & \mathbf{M}_{ii} & \mathbf{0} \\ \mathbf{0} & \mathbf{0} & \mathbf{M}_{ss} \end{bmatrix} \begin{Bmatrix} \ddot{\mathbf{u}}_p \\ \ddot{\mathbf{u}}_i \\ \ddot{\mathbf{u}}_s \end{Bmatrix} + \begin{bmatrix} \mathbf{C}_{pp} & \mathbf{C}_{pi} & \mathbf{0} \\ \mathbf{C}_{ip} & \mathbf{C}_{ii} & \mathbf{C}_{is} \\ \mathbf{0} & \mathbf{C}_{si} & \mathbf{C}_{ss} \end{bmatrix} \begin{Bmatrix} \dot{\mathbf{u}}_p \\ \dot{\mathbf{u}}_i \\ \dot{\mathbf{u}}_s \end{Bmatrix} + \begin{bmatrix} \mathbf{K}_{pp} & \mathbf{K}_{pi} & \mathbf{0} \\ \mathbf{K}_{ip} & \mathbf{K}_{ii} & \mathbf{K}_{is} \\ \mathbf{0} & \mathbf{K}_{si} & \mathbf{K}_{ss} \end{bmatrix} \begin{Bmatrix} \mathbf{u}_p \\ \mathbf{u}_i \\ \mathbf{u}_s \end{Bmatrix} = - \begin{bmatrix} \mathbf{M}_{pp} & \mathbf{0} & \mathbf{0} \\ \mathbf{0} & \mathbf{M}_{ii} & \mathbf{0} \\ \mathbf{0} & \mathbf{0} & \mathbf{M}_{ss} \end{bmatrix} \begin{Bmatrix} \mathbf{0} \\ \mathbf{0} \\ \ddot{\mathbf{u}}_g \end{Bmatrix} \tag{13}$$

where **M**, **C** and **K** are the mass, damping and stiffness matrices obtained by the finite-element formulation. The common nodes at the interface of the pipeline and soil or springs representing side regions soil are defined with "*i*"; the nodes of shell elements representing the pipeline and the nodes within the soil around the pipeline in the middle part are defined with "*p*" and "*s*", respectively. The mass, the stiffness and the damping at the interface nodes are the sum of the contribution from the pipeline (*p*) and the soil (*s*), and are given by

$$\mathbf{M}_{ii} = \mathbf{M}_{ii}^{p} + \mathbf{M}_{ii}^{s} \quad ; \mathbf{C}_{ii} = \mathbf{C}_{ii}^{p} + \mathbf{C}_{ii}^{s} \quad \text{and}$$
$$\mathbf{K}_{ii} = \mathbf{K}_{ii}^{p} + \mathbf{K}_{ii}^{s} \tag{14}$$

As it was noted the liquefiable part of the soil can experience very large amount of strains during the earthquake. Having this kind of non-linearity and also the material and geometric non-linearities of the pipe, using implicit algorithm can be followed with some difficulties in terms of convergences. Therefore, in this study, the explicit approach as a computational efficient approach was adopted to solve the governing equations. The static geometric non-linear analysis under the static situation is essential as a starting point for the non-linear seismic analysis using explicit algorithm, taking the initial conditions at rest for the soil and accounting the initial induced strains to the pipeline due to surcharge loads. The explicit central-difference operator satisfies the dynamic equilibrium equations at the beginning of the increment, *t*; The accelerations calculated at time t are used to advance the velocity solution to time $t+\frac{\Delta t}{2}$ and the displacement solution to time $t+\Delta t$ as

$$\{\dot{u}\}^N_{i+\frac{1}{2}} = \{\dot{u}\}^N_{i-\frac{1}{2}} + \frac{\Delta t_{i+1} + \Delta t_i}{2} \{\ddot{u}\}^N_i \tag{15}$$

$$\{u\}^N_{i+1} = \{u\}^N_i + \Delta t_{i+1} \{\dot{u}\}^N_{i+\frac{1}{2}} \tag{16}$$

The subscript *i* refers to the increment number in an explicit dynamics step. $\{u\}^N$ is the displacement vector, $\{\dot{u}\}^N$ is the velocity vector and $\{\ddot{u}\}^N$ is the acceleration vector, where *N* is the number of degrees of freedom in the model. The explicit integration rule is quite simple but by itself does not provide the computational efficiency associated with the explicit dynamics procedure. The accelerations at the beginning of the time increment using D'Alambert's principle are computed by

$$\{\ddot{u}\}^N_i = [M]^{-1\,NJ} (\{P\}^J_i - \{I\}^J_i) \tag{17}$$

where $[M]^{-1\,NJ}$ is the inverse mass matrix, $\{P\}^J_i$ is the applied load vector, and $\{I\}^J_i$ is the internal force vector including stiffness and damping forces and *J* is a numerator. A lumped mass matrix is used because its inverse is simple to compute and because the vector multiplication of the mass inverse by the inertial force requires only *N* operations. The explicit procedure requires no iterations and no tangent stiffness matrix. The internal force vector, $\{I\}^J_i$ is assembled from contributions from the individual elements such that a global stiffness matrix need not be formed. The explicit procedure integrates through time by using many small time increments. The central-difference operator is conditionally stable, and the stability limit for the operator (with no damping) is given in terms of the highest frequency of the system as

$$\Delta t \le \frac{2}{\omega_{\max}} \tag{18}$$

With damping, the stable time increment is given by

$$\Delta t \le \frac{2}{\omega_{\max}} (\sqrt{1 + \zeta_{\max}^{\,2}} - \zeta_{\max}) \tag{19}$$

where $\omega_{\max}$ is the highest natural frequency and $\zeta_{\max}$ is the fraction of critical damping in the mode with the highest frequency.

EXAMPLE CALCULATIONS

To investigate the effect of liquefaction on seismic behavior of buried pipelines, using the model developed in this study, a gas pipeline with a diameter of 610 mm, 50m length and 9.5 mm wall thickness was used. The liquefaction zone assumed to spread along a 10m length of the pipeline. The liquefiable zone is designed with a 7m-width and 8m-depth uniform saturated sandy soil space, ground water is set at the ground

surface; and the steel pipe assumed to be buried at the depth of 1.5m. Table 2 shows the soil dynamic parameters used in the example.

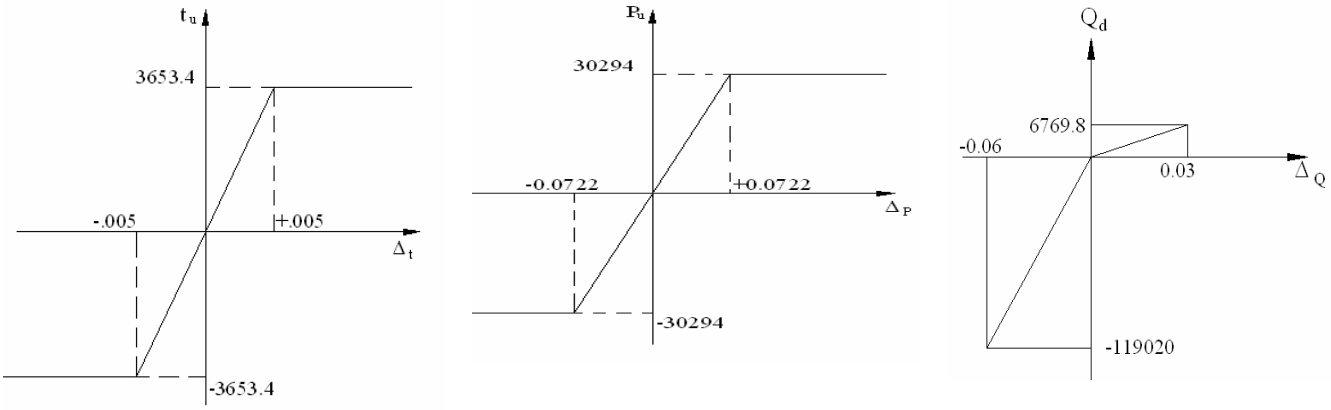

Fig. 5. Bilinear soil-pipeline interaction relationships

Table 2. Soil Dynamic Parameters

Soil Parameters	Density	ϕ	ν	E_0	Interface friction Angle
	1450	30	0.45	0.9	21

Fig. 5 shows the bilinear force-displacement relationships representing the axial, transverse horizontal and transverse vertical soil stiffnesses in the non-liquefiable side parts. To take into account the non-linear behavior of the pipe, steel Type X-60 with Ramberg-Osgood elastoplastic stress-strain relationship was used. The dynamic analyses of the soil-pipeline system was carried subjected to Northridge Earthquake (1994) followed by the static analysis for the at rest condition under gravity loads. The ground excitation is applied to the bottom boundary conditions horizontally. The boundary adopts Lysmer viscous boundary, which can eliminate the numerical error aroused by the limited region. Besides, the pore water pressure boundary is designed as a complete drain boundary.

For the Northridge earthquake excitation, Figs. 6 and 7 show the development of pore water pressure changes with the seismic duration for different depths (element A at the depth of 2m and element B at the depth of 7m). From the results of Figs. 6 and 7 for the system studied in this paper, the liquefaction will happen after 8s of the earthquake (the first 7s is related to the static loading). It can be seen that after liquefaction occurred the soil strains raise significantly leading to remarkable settlements in the soil-pipeline system (Fig. 11). At the shallow depths, as the cyclic strength decreases, pore pressures developed faster and then it can be noted after the initial liquefaction, the maximum shear strain increase significantly. Fig. 8 shows the variation of maximum shear strain during the excitation for the element A. This figure also shows after around 8 seconds of the earthquake, the loss of strength starts to take place as pore water pressure builds up.

The stress components for two elements A and B are shown in Figs. 9 and 10. The results indicated that amount of shear strain that can develop or the amount of loss of shear stress appears to be related by the number of cycles and their magnitude, which occurs in the stress time history after the application of peak stress.

To consider the liquefaction effect on deformation of the pipeline, the longitudinal settlement of the pipe is recorded for the 8s of the earthquake. It can be noted from Fig. 12 the general tendency for deformation of the pipe are similar suggested by ALA as

$$y(x) = \delta/2\,(1-\cos n\pi x/L) \qquad (20)$$

CONCLUSION

In this paper, an effective stress method and nonlinear constitutive relation model of soil were used to study the development and the dissipation of pore water pressure during a seismic excitation. This very simple algorithm to define the hysteretic loops for liquefiable sands during loading-reloading phase of excitation was implemented into the finite element method. A 3D soil-pipeline model was developed to study the

dynamic behavior of pipelines embedded in liquefiable soils. A suitable contact interface model is adopted to simulate the interaction between pipeline and surrounding soil. Using the 3D methodology developed in this study, a numerical simulation of the full-process liquefaction analysis for an underground pipeline was performed. The results show that the methodology can predict the pore pressure build-up and consequently the loss of soil strength consistent with the liquefaction process. The deformation induced in the pipeline due to liquefaction was found similar to a harmonic settlement.

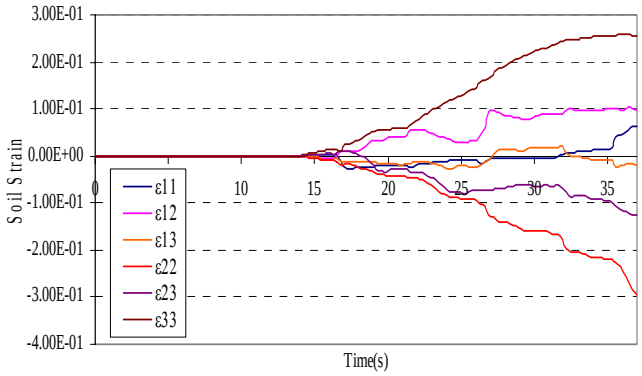

Fig. 6. Strains time histories for A-1 element

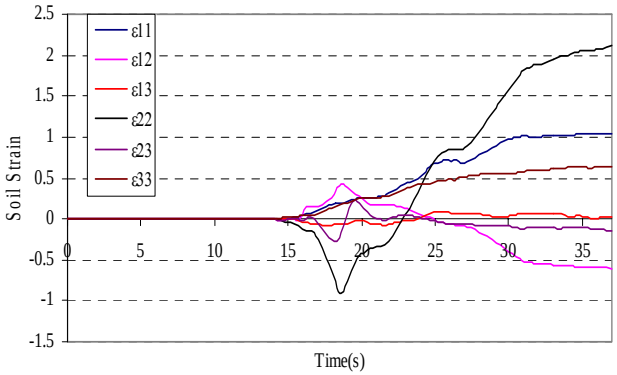

Fig. 7. Strains time histories for A-2 element

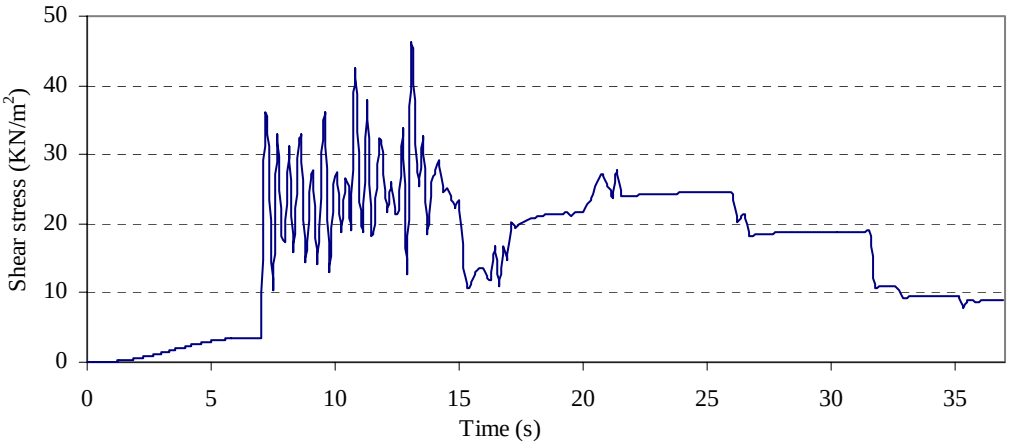

Fig. 8. Maximum shear stress on saturated soil

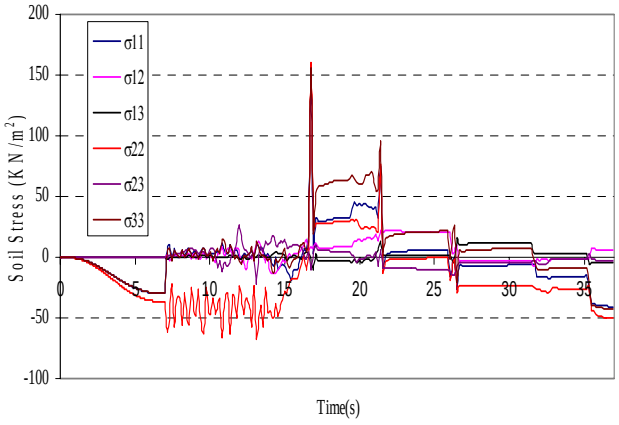

Fig. 9. Stresses time histories for A-1 element

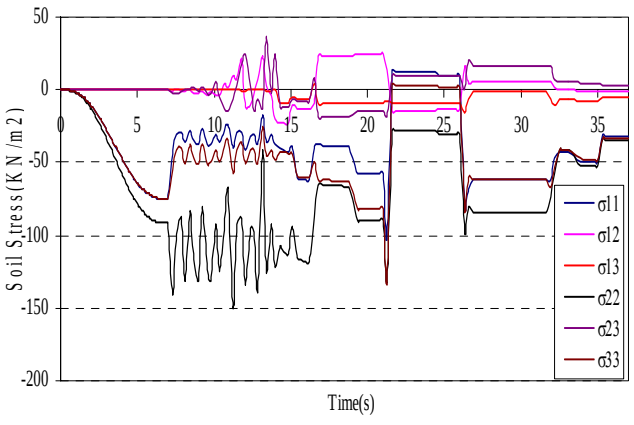

Fig. 10. Stresses time histories in A-2 element

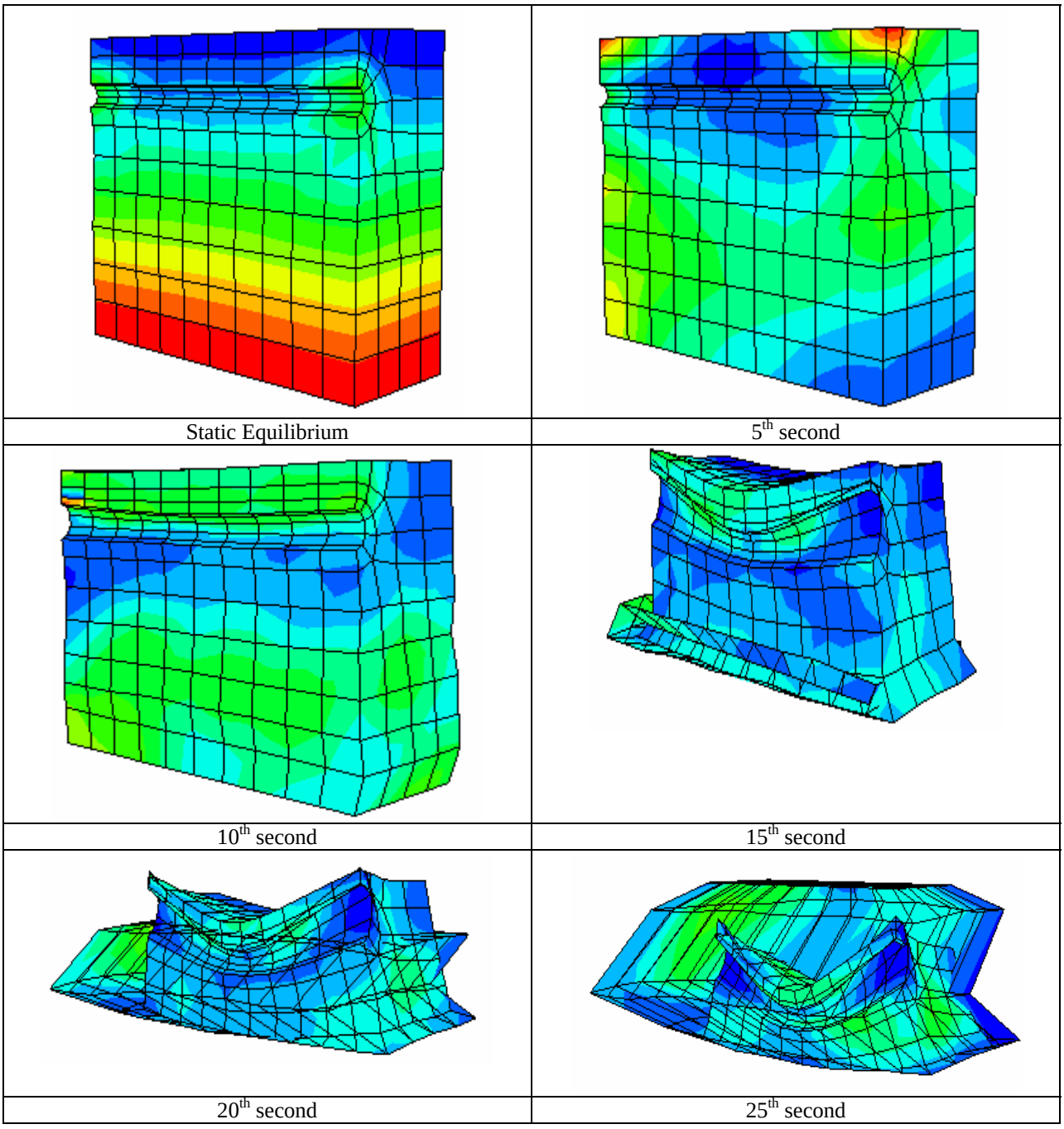

Fig. 11. The soil-pipeline deformation during earthquake excitation

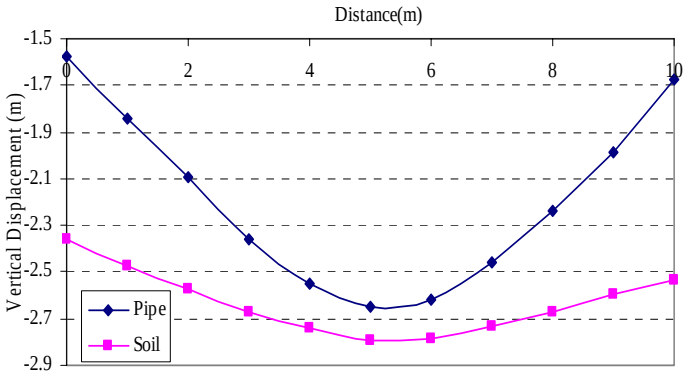

Fig. 12. The pipe deformation during the liquefaction at 8s of earthquake

ACKNOWLEDGEMENT

This research was funded by by Isfahan Gas Distribution Company as part of project to evaluate the serviceability of Isfahan Gas network during extreme events. Their support is greatly appreciated.

REFERENCES

American Lifelines Alliance – ASCE [2001], "*Guidelines for the Design of Buried Steel Pipes*".

Ariman, T. and Lee B. J. [1992], "Tension/Bending Behavior of Buried Pipe-lines Subjected to Fault Movements in Earthquake", *Proceeding 10th World Conference on Earthquake Engineering*, Madrid, pp. 5423-5426.

Habte, M. A. [2006], "Numerical and Constitutive Modeling Of Monotonic and Cyclic Loading in Variably Saturated Soils, *Ph.D. Thesis*, School of Civil and Environmental Engineering, The University of New South Wales, Sydney, Australia.

Finn, W. D. and Lee, W. [1977], "An Effective Stress Model For Liquefaction", *ASCE Journal, Geotechnical Engineering Division*, GT.6, pp. 517-533.

Kennedy, R. P., Chow, A. W. and Williamson, R. A. [1977], "Fault Movement Effects on Buried Oil Pipeline", *Transportation Engineering Journal*, ASCE, Vol. 103, No. 5, pp. 617-633.

Newmark, N. M. and Hall, W. J., [1975], "Pipeline Design to Resist Large Fault Displacement", *Proceeding of U. S. National Conference on Earthquake Engineering*, pp. 2416-2425.

O'Rourke, T. and Lane, P. [1989], "Liquefaction Hazards and Their Effects on Buried Pipelines", *NCEER*, pp. 89-007.

Prakash, S. [1981], "*Soil Dynamics*". McGraw-Hill, Inc.

Trautmann, C. H. and O'Rourke, T.D. [1983], "Behavior of pipe in dry sand under lateral and uplift loading", *Geotechnical Engineering Report 83-7, Cornell University.*

Wang L., R., L., and Yeh Y. [1985], "A Refined Seismic Analysis and Design of Buried Pipeline for Fault Movement", *Earthquake Engineering and Structural Dynamics*, vol. 13, 75-96.